

GALAXY CLUSTER ASSEMBLY AT $Z = 0.37$ ¹

ANTHONY H. GONZALEZ^{2,3}, KIM-VY H. TRAN⁴, MICHELLE N. CONBERE³, & DENNIS ZARITSKY⁵

Accepted to The Astrophysical Journal Letters

ABSTRACT

We present X-ray and spectroscopic confirmation of a cluster assembling from multiple, distinct galaxy groups at $z = 0.371$. Initially detected in the Las Campanas Distant Cluster Survey, the structure contains at least four X-ray detected groups that lie within a maximum projected separation of 4 Mpc and within $\Delta v = 550 \text{ km s}^{-1}$ of one another. Using *Chandra* imaging and wide-field optical spectroscopy, we show that the individual groups lie on the local $\sigma - T$ relation, and derive a total mass of $M \geq 5 \times 10^{14} M_{\odot}$ for the entire structure. We demonstrate that the groups are gravitationally bound to one another and will merge into a single cluster with $\gtrsim \frac{1}{3}$ the mass of Coma. We also find that although the cluster is in the process of forming, the individual groups already have a higher fraction of passive members than the field. This result indicates that galaxy evolution on group scales is key to developing the early-type galaxies that dominate the cluster population by $z \sim 0$.

Subject headings: galaxies: evolution — galaxies: clusters: general — X-rays: galaxies: clusters

1. INTRODUCTION

A fundamental prediction of hierarchical structure formation is that galaxy clusters assemble at late times from the merging and accreting of smaller structures (Peebles 1970). While many examples of the accretion of groups and galaxies onto massive clusters exist (e.g. Abraham et al. 1996; Hughes & Birkinshaw 1998; Tran et al. 2005), we lack clear early-stage examples of clusters being assembled from an ensemble of galaxy groups. The identification of such proto-clusters is challenging due to the extensive mapping required to trace the substructure that will eventually form the cluster.

Nonetheless, detection of these rare systems is well worth the effort. They provide a detailed snapshot of the process of filamentary collapse and assembly in the quasi-linear regime, and enable a *direct* study of a class of progenitors that does not yet include a massive cluster. The latter is particularly critical for determining if “pre-processing” in groups is responsible for the bulk of the observed differences in morphology and stellar populations between cluster and field galaxies (Zabludoff & Mulchaey 1998; Kodama et al. 2001)

We present confirmation of a protocluster identified optically in the Las Campanas Distant Cluster Survey (LCDCS; Gonzalez et al. 2001). Designed to provide a catalog of clusters at $z \approx 0.35 - 0.9$, the LCDCS extends down to group masses at the lowest redshifts and hence can be used to identify filamentary structures at $z \sim 0.4$. One such candidate structure includes four LCDCS candidates within a $3.5'$ radius region with estimated redshifts of $z_{est} = 0.35 - 0.50$. We demonstrate that we are witnessing the assembly of a cluster from what can be described in analogy to superclusters as a supergroup. Throughout this paper, we use a standard cosmology ($\Omega_M = 0.3$, $\Omega_{\Lambda} = 0.7$, $H_0 = 70 \text{ km s}^{-1}$).

2. X-RAY OBSERVATIONS WITH CHANDRA

The target field was observed with *Chandra* ACIS-I in Very Faint (VF) mode on March 24, 2002 (Obs ID 3235) for 70.13 ks, with the detector oriented such that one LCDCS candidate was imaged in each ACIS-I chip. Data reduction was performed in the standard fashion using CIAO 3.0. The level 1 event file was reprocessed to correct for charge transfer inefficiency and to reduce the VF mode particle background,⁶ and bad pixels and events with bad grades were removed in the standard fashion. Strong flares were removed using the `lc_clean` routine written by Maxim Markevitch, yielding a net exposure time of 64 ks. The high energy background in the remaining time interval is consistent with the quiescent rate from the “blank-sky” background file to within 1%.⁷

Image analysis is performed in the 0.8-3 keV band. Using wavelet detection, we identify six distinct extended sources at $> 5\sigma$ significance (Figure 1). Four of these sources are coincident to within $10''$ with LCDCS candidates, while the other two extended sources have no LCDCS counterparts. One of these latter two (source 5) could not have been detected by the LCDCS due to its proximity to a bright star; the other is the faintest of the six sources and appears to be a very poor group.

Spectral analysis is performed in the 0.7-8 keV band. Temperatures are measured within 400 kpc circular apertures to maximize signal-to-noise (S/N), excluding point sources, and using the appropriately normalized ACIS “blank-sky” file for the background. We fit the spectra using a MEKAL model, with the absorption fixed to the galactic value $n_H = 5.13 \times 10^{20} \text{ cm}^{-2}$ and the metal abundance fixed at $Z = 0.3$ (Mushotzky & Loewenstein 1997). For four of the extended sources, we fix the redshift to the median velocity of the associated galaxies (see §3), while for LCDCS 0259 (source 2), which lies outside the spectroscopic survey region, we use the single redshift obtained for the brightest associated galaxy. The best-fit temperatures (Table 1, with 68% uncertainties) range from $T = 1.7 - 3 \text{ keV}$ and are consistent with the temperatures found for groups or poor clusters similar to Virgo (Shibata et al. 2001). Only for the faintest source do we lack sufficient S/N to obtain a temperature.

¹ Based on observations with the Chandra X-ray Observatory, the VLT (program 072.A-0367), the Magellan Baade telescope, and the MMT Observatory, a joint venture of the Smithsonian Astrophysical Observatory and the University of Arizona.

² NSF Astronomy and Astrophysics Postdoctoral Fellow

³ Department of Astronomy, University of Florida, Gainesville, FL 32611

⁴ Institute for Astronomy, ETH Zürich, CH-8093 Zürich, Switzerland

⁵ Steward Observatory, University of Arizona, 933 North Cherry Avenue, Tucson, AZ 85721

⁶ See http://cxc.harvard.edu/cal/Acis/Cal_prods/vfbkgrnd/

⁷ See <http://cxc.harvard.edu/ciao/threads/acisbackground/>

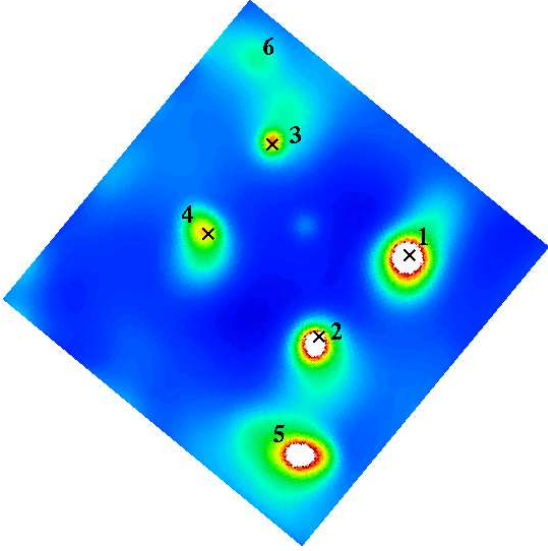


FIG. 1.— Smoothed X-ray map ($13.2' \times 13.2'$) of the structure with point sources excised; north is up and east is to the left. The crosses denote the locations from the LCDCS catalogs and the numeric labels correspond to the designations in Table 1. Redshifts have been obtained for sources 1-5.

3. OPTICAL SPECTROSCOPY

3.1. MMT, Magellan, and VLT Observations

To confirm that the X-ray sources are part of a larger structure, long-slit spectra of the candidate brightest group galaxies (BGGs) associated with each of the six X-ray peaks were obtained with Magellan and the MMT in February and April 2003, respectively. Redshifts obtained for the BGG's in groups 1-5 confirm that at least four of the X-ray regions are associated with a single physical complex at $z = 0.37$. Only the BGG candidate for group 1 was found to lie at a different redshift ($z = 0.48$). These initial results motivated a more extensive spectroscopic program with the VLT.

Using VIMOS (LeFevre et al. 2003), we measure redshifts and determine membership for galaxies near groups 1, 3, 4, and 5; group 2 was excluded due to an interchip gap. From a $14' \times 16'$ R-band image (1820s) taken with VIMOS, we generated a catalog of ~ 2100 objects with $R \leq 22.5$. Our observations used three multi-slit masks with $1''$ -wide slits and targeted 443 of these objects; each mask had a total integration time of 2400 seconds. While ours is a magnitude limited survey and targets were not selected by morphology, preference was given to objects in visually overdense regions. The intermediate resolution (MR) grism on VIMOS gave us a spectral range of $0.5 - 1.0 \mu\text{m}$ and spectral resolution of 12.2 \AA .

To reduce and extract spectra, we use a combination of IRAF⁸ routines and custom software provided by D. Kelson (Kelson 1998); a more detailed explanation of the reduction pipeline can be found in Tran et al. (2005). We use a spectrophotometric standard to correct for the telluric A and B bands and flux calibrate the spectra.

We determine redshifts with the IRAF cross-correlation routine XCSAO (Kurtz et al. 1992). Our final redshift catalog has 413 objects, corresponding to a target success rate of

⁸ IRAF is distributed by the National Optical Astronomy Observatories, which are operated by the Association of Universities for Research in Astronomy, Inc., under cooperative agreement with the National Science Foundation.

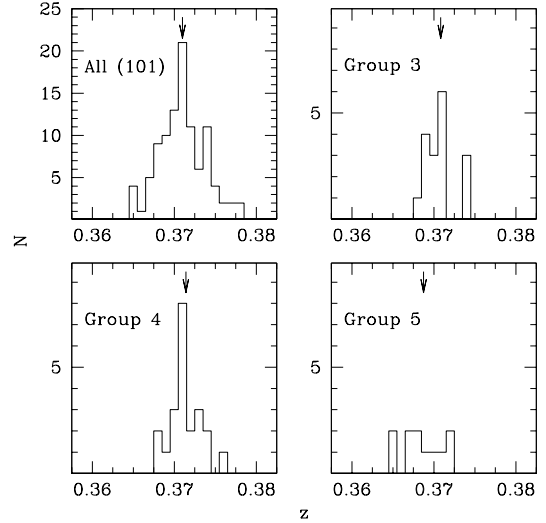


FIG. 2.— *Top left* – Redshift distribution of the 101 confirmed members (defined by $0.36 < z < 0.38$) in SG1120-1202 ($z = 0.3710 \pm 0.0004$). Although the members trace a very large structure (projected spatial distance ~ 4 Mpc) and include galaxies from 3 of the groups at $z = 0.37$, they have a remarkably narrow redshift distribution and a velocity dispersion of only $\sigma = 616 \pm 50 \text{ km s}^{-1}$. *Top right and lower panels* – Redshift distributions for the individual groups; the arrow denotes the average redshift of the members. To isolate members of each individual group, here we consider only members within 500 kpc of the X-ray centers. Even with our conservative selection criterion, the maximum redshift difference between the groups is only $\Delta z = 0.0025$.

93%. The average redshift uncertainty estimated by XCSAO is $\sim 30 \text{ km s}^{-1}$; while XCSAO tends to underestimate the errors, this problem does not affect our results.

3.2. Redshift Distribution

From spectroscopy of 4 of the 6 regions with extended X-ray emission, we identify a peak corresponding to LCDCS 0258 ($z = 0.48$, source 1), and another corresponding to three X-ray groups at $z = 0.37$, hereafter referred to as SG1120-1202 (SG standing for “supergroup”). The mean redshift of the 101 galaxies belonging to SG1120-1202 is $z = 0.3710 \pm 0.0004$. Although the members lie in multiple, distinct X-ray bright regions and trace a large structure with a projected spatial distance of ~ 4 Mpc, their redshift distribution is remarkably narrow (Fig. 2 and Table 1) and their velocity dispersion surprisingly small ($\sigma = 616 \pm 50 \text{ km s}^{-1}$). The mean redshift, velocity dispersion, and associated errors are determined using the biweight and jackknife methods (Beers et al. 1990). To compare the dynamics of the three X-ray groups to each other, members of each group are selected as galaxies that lie within 500 kpc of their respective X-ray peak. The redshift distributions of the three groups are shown in Figure 2 and their velocity dispersions are listed in Table 1.

3.3. Spectral Populations in SG1120-1202

To quantify the recent star formation histories of galaxies in SG1120-1202, we separate the members by [OII] equivalent width into absorption ([OII] $\lambda 3727 < 5 \text{ \AA}$; “passive”) and emission ([OII] $\lambda 3727 \geq 5 \text{ \AA}$; “active”) line galaxies. We use the same bandpasses as in Fisher et al. (1998) to measure the [OII] doublet, and our wavelength coverage includes the [OII] doublet for 95 of the 101 confirmed members.

TABLE 1. GROUP SAMPLE

ID	α (J2000)	δ (J2000)	LCDCS ID	z	T (keV)	σ km s ⁻¹	N_g^a
1	11:19:55.2	-12:02:28	0258	0.4794	$2.3^{+0.4}_{-0.3}$	820 ± 101	17
2	11:20:07.6	-12:05:13	0259	0.3707	$2.2^{+0.7}_{-0.4}$	—	1
3	11:20:13.2	-11:58:44	0260	0.3704	$1.7^{+0.5}_{-0.3}$	369 ± 76	17
4	11:20:22.3	-12:01:45	0264	0.3713	$1.8^{+1.2}_{-0.5}$	446 ± 83	22
5	11:20:10.0	-12:08:50	—	0.3688	$3.0^{+1.2}_{-1.0}$	557 ± 93	11
6	11:20:15.6	-11:56:03	—	—	—	—	—

^aNumber of galaxies used to calculate the mean redshift and velocity dispersion.

The fraction of passive galaxies in SG1120-1202 is $61 \pm 8\%$. This fraction is less than in CL 1358+62 ($81 \pm 6\%$), a more massive cluster at comparable redshift ($z = 0.33$, $\sigma = 1027$ km s⁻¹; Fisher et al. 1998), but twice as high as the field value ($27 \pm 4\%$ at $0.2 < z < 0.5$; Tran et al. 2004). The passive galaxy fraction in SG1120-1202 most closely resembles that found in X-ray luminous groups in the nearby universe ($69 \pm 7\%$; Tran et al. 2001). Direct comparison to these other samples is valid because all four are magnitude-selected and use the same [OII] selection criteria.

4. CLUSTER ASSEMBLY

SG1120-1202's extended, roughly linear geometry is seen in both its X-ray emission and the spatial distribution of its galaxies. Coupled with the small dispersion in the mean group redshifts ($\Delta z = 0.0025$) and visible signs of interaction in the X-ray map (groups 2+5 and 3+6), this geometry argues that we are witnessing the initial stages of filamentary collapse and the formation of a more massive cluster. To test this hypothesis, we estimate SG1120-1202's total mass, assess the probability that the system is bound, and estimate the dynamical timescale for the system to merge. We include groups 2-5 in this analysis; we are confident that group 2 is part of the complex despite having only one redshift, both because the redshift is for the BGG (a $3 L_*$ elliptical within $3''$ of the X-ray peak) and because asymmetry in the X-ray map indicates that groups 2 and 5 are interacting.

4.1. Total Mass

Given the consistency of the groups with the local $\sigma - T$ relation (Figure 3), we assume hydrostatic equilibrium and use the local mass-temperature ($M - T$) relation in Shimizu et al. (2003, Equation 16) to estimate the masses of the individual groups.⁹ The four spectroscopically confirmed groups at $z = 0.37$ have $T = 1.7 - 3$ keV, yielding a combined mass of $M = 5.3^{+1.6}_{-0.9} \times 10^{14} M_\odot$. This mass is a lower limit on the total mass of the system because it does not include group 6, groups that may lie outside the *Chandra* field, or material in filaments between groups. It is equivalent to that of a single cluster with $T \sim 5$ keV, and at least a third the mass of the Coma cluster (Hughes 1989; Honda et al. 1996).

4.2. Dynamical State

That the individual groups in SG1120-1202 lie on the local $\sigma - T$ relation argues that each group is approximately virialized and that, if the larger structure is bound, the groups are

⁹ Evolution in the $M - T$ relation should be negligible over this redshift interval (Ettori et al. 2004).

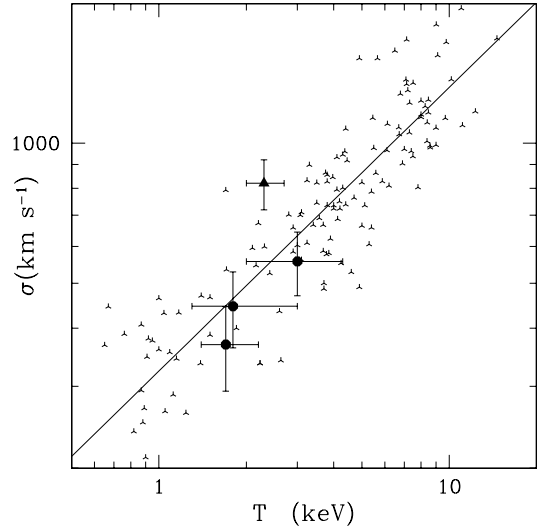


FIG. 3.— Comparison of the groups in this study with the local $\sigma - T$ relation (Xue & Wu 2000). The solid symbols with error bars correspond to the groups in our sample, circles denoting members of the supergroup ($z = 0.37$) and the triangle LCDCS 0258 ($z = 0.48$, source 1). The other points are the local data from Xue & Wu (2000) and the solid line is their best fit for this combined group and cluster sample. Our sample is consistent with this local relation.

infalling for the first time. We perform a simple dynamical analysis to assess the likelihood that the SG1120-1202 complex is indeed gravitationally bound.

The individual groups will be bound to the larger system if

$$\frac{GM}{R_p(\sin i)^{-1}} \geq \frac{v_{pec}^2}{2} \quad (1)$$

where M is the total mass, v_{pec} is the pairwise peculiar velocity for groups, R_p is the projected distance between the groups, and i is the opening angle. We assume the local value of $\langle v_{pec} \rangle = 325 \pm 175$ km s⁻¹ from Padilla et al. (2001) and conservatively take $R_p = 3$ Mpc; this value corresponds to the largest separation between the X-ray groups.

Using our X-ray estimate of the total mass, the above inequality holds for $i \gtrsim 4^\circ$. Geometrically, the probability is 99.5% that the opening angle is at least this large. Even assuming $v_{pec} = 500$ km s⁻¹ (1σ above the mean value from Padilla et al. 2001), the inequality holds for $i \gtrsim 10^\circ$ and the probability that the groups are bound remains high (97%).

The above analysis indicates that an unbound system is unlikely, but does not conclusively eliminate the possibility. We can strengthen the constraint by exploring the implications of an unbound system. For $i \lesssim 10^\circ$, the groups are separated by $\gtrsim 20$ Mpc, and the corresponding Hubble flow redshift offset is $(\Delta z)_H \gtrsim 0.0075$ (2250 km s⁻¹). In this case, $(\Delta z)_H$ is a factor of three greater than the observed maximum redshift separation between the groups. Thus relative peculiar velocities of $\gtrsim 1500$ km s⁻¹ would be required to counterbalance the Hubble flow and explain the small observed redshift separation; this is an implausibly large value if the groups are truly separated by $\gtrsim 20$ Mpc and not infalling.

We conclude that the groups in SG1120-1202 are bound to each other. The dynamical time for this system is

$$t_{dyn} \approx \sqrt{\frac{R^3}{GM}} \approx 1.2(\sin i)^{-3/2} \text{ Gyrs}, \quad (2)$$

for $R_p = 1.5$ Mpc and $M = 5 \times 10^{14} M_\odot$. For $i \gtrsim 26^\circ$, t_{dyn} is less than the lookback time.

An alternative treatment is to assume that the groups are bound and on radial orbits that have not yet crossed the center of the potential, and use the timing argument (Kahn & Woltjer 1959) to determine their line-of-sight distance by fitting the projected separation and radial velocity in the center of mass frame. For the four groups we find solutions with line-of-sight distances from the center-of-mass of between 7.5 and 10 Mpc. These solutions have $11^\circ < i < 27^\circ$, and hence suggest that the complete collapse of the system will occur after the current time. The main conclusion from this analysis is that a bound solution exists with the measured masses that can reproduce the positions and radial velocities of the groups. Detailed descriptions of the orbits and future merger history require more information.

5. CONCLUSIONS

Our observations confirm that SG1120-1202 is a protocluster being built up by the assembly of multiple galaxy groups. From deep *Chandra* imaging and optical spectroscopy, we find that SG1120-1202 contains a minimum of four X-ray luminous groups at $z = 0.371$ within a projected 4 Mpc of one another. The groups have X-ray temperatures of $T = 1.7 - 3$ keV and their mean redshifts span a narrow range of $\Delta z = 0.0025$ (550 km s^{-1}). The group velocity dispersions and X-ray temperatures fall on the local $\sigma - T$ relation, indicating that they are each virialized systems with a combined mass $M \geq 5 \times 10^{14} M_\odot$. Using dynamical arguments, we demon-

strate that the X-ray groups are gravitationally bound to one another and should merge into a single cluster; the resulting cluster will have $\gtrsim \frac{1}{3}$ the mass of Coma.

While SG1120-1202 represents only one of a variety of accretion histories that can yield a moderate mass cluster at $z = 0$, this assembly path – the late merging of multiple roughly equal mass subhalos – is of particular interest. SG1120-1202 provides a unique laboratory for assessing the impact of local density upon the evolution of member galaxies, and for quantifying the degree to which the group environment acts to “pre-process” galaxies prior to cluster assembly. Already we see that the individual groups have twice as many passive galaxies as the field, indicating that galaxy evolution on group scales is key to developing the early-type galaxies that dominate the cluster population by $z \sim 0$.

We are indebted to A. Vikhlinin and M. Markevitch for their assistance and for providing us with codes employed in the *Chandra* analysis. Support for this work was provided by NASA through Chandra Award GO2-3183X3 issued by the CXO Center, which is operated by SAO for and on behalf of NASA under contract NAS8-03060. AHG is funded by an NSF Astronomy & Astrophysics Postdoctoral Fellowship under award AST=0407085, KT acknowledges support from the Swiss National Science Foundation, and DZ acknowledges fellowships from the David and Lucile Packard Foundation and Alfred P. Sloan Foundation.

REFERENCES

- Abraham, R. G., Smecker-Hane, T. A., Hutchings, J. B., Carlberg, R. G., Yee, H. K. C., Ellingson, E., Morris, S., Oke, J. B., & Rigler, M. 1996, *ApJ*, 471, 694
- Beers, T. C., Flynn, K., & Gebhardt, K. 1990, *AJ*, 100, 32
- Ettori, S., Borgani, S., Moscardini, L., Murante, G., Tozzi, P., Diaferio, A., Dolag, K., Springel, V., Tormen, G., & Tornatore, L. 2004, *MNRAS*, 354, 111
- Fisher, D., Fabricant, D., Franx, M., & van Dokkum, P. 1998, *ApJ*, 498, 195+
- Gonzalez, A. H., Zaritsky, D., Dalcanton, J. J., & Nelson, A. 2001, *ApJS*, 137, 117
- Honda, H., Hirayama, M., Watanabe, M., Kunieda, H., Tawara, Y., Yamashita, K., Ohashi, T., Hughes, J. P., & Henry, J. P. 1996, *ApJ*, 473, L71+
- Hughes, J. P. 1989, *ApJ*, 337, 21
- Hughes, J. P. & Birkinshaw, M. 1998, *ApJ*, 497, 645
- Kahn, F. D. & Woltjer, L. 1959, *ApJ*, 130, 705
- Kelson, D. D. 1998, Ph.D. thesis, University of California at Santa Cruz (Santa Cruz, CA: University of California)
- Kodama, T., Smail, I., Nakata, F., Okamura, S., & Bower, R. G. 2001, *ApJ*, 562, L9
- Kurtz, M. J., Mink, D. J., Wyatt, W. F., Fabricant, D. G., Torres, G., Kriss, G. A., & Tonry, J. L. 1992, in *Astronomical Data Analysis Software and Systems I*, ed. d. M. Worrall, C. Biemesderfer, & J. Barnes, Vol. 25 (A.S.P. Conference Series), 432
- LeFevre, O., Saisse, M., Mancini, D., & et al. 2003, in *Proceedings of the SPIE*, Volume 4841, pp. 1670-1681.
- Mushotzky, R. F. & Loewenstein, M. 1997, *ApJ*, 481, L63+
- Padilla, N. D., Merchán, M. E., Valotto, C. A., Lambas, D. G., & Maia, M. A. G. 2001, *ApJ*, 554, 873
- Peebles, P. J. E. 1970, *AJ*, 75, 13
- Shibata, R., Matsushita, K., Yamasaki, N. Y., Ohashi, T., Ishida, M., Kikuchi, K., Böhringer, H., & Matsumoto, H. 2001, *ApJ*, 549, 228
- Shimizu, M., Kitayama, T., Sasaki, S., & Suto, Y. 2003, *ApJ*, 590, 197
- Tran, K. H., Franx, M., Illingworth, G. D., van Dokkum, P., Kelson, D. D., & Magee, D. 2004, *ApJ*, 609, 683
- Tran, K. H., Simard, L., Zabludoff, A. I., & Mulchaey, J. S. 2001, *ApJ*, 549, 172
- Tran, K. H., van Dokkum, P., Illingworth, G. D., Kelson, D., Gonzalez, A., & Franx, M. 2005, *ApJ*, 619, 134
- Xue, Y. & Wu, X. 2000, *ApJ*, 538, 65
- Zabludoff, A. I. & Mulchaey, J. S. 1998, *ApJ*, 496, 39